Published in final edited form as:
Acta Biomater. 2012 September ; 8(9): 3436–3445. doi:10.1016/j.actbio.2012.05.016.

Human embryonic stem cell-encapsulation in alginate microbeads in macroporous calcium phosphate cement for bone tissue engineering

Minghui Tang[1], **Wenchuan Chen**[1], **Michael D. Weir**[1], **Wahwah Thein-Han**[1], and **Hockin H. K. Xu**[1,2,3,4,*]

[1]Biomaterials & Tissue Engineering Division, Dept. of Endodontics, Prosthodontics and Operative Dentistry, University of Maryland Dental School, Baltimore, MD 21201

[2]Center for Stem Cell Biology & Regenerative Medicine University of Maryland School of Medicine, Baltimore, MD 21201

[3]University of Maryland Marlene and Stewart Greenebaum Cancer Center University of Maryland School of Medicine, Baltimore, MD 21201

[4]Dept. of Mechanical Engineering, University of Maryland, Baltimore County, MD 21250

Abstract

Human embryonic stem cells (hESCs) are exciting for regenerative medicine applications because of their strong proliferative ability and multilineage differentiation capability. To date there has been no report on hESC seeding with calcium phosphate cement (CPC). The objective of this study was to investigate hESC-derived mesenchymal stem cell (hESCd-MSC) encapsulation in hydrogel microbeads in macroporous CPC for bone tissue engineering. hESCs were cultured to form embryoid bodies (EBs), and the MSCs were then migrated out of the EBs. hESCd-MSCs had surface markers characteristic of MSCs, with positive alkaline phosphatase (ALP) staining when cultured in osteogenic medium. hESCd-MSCs were encapsulated in alginate at a density of 1 million cells/mL, with an average microbead size of 207 μm. CPC contained mannitol porogen to create a porosity of 64% and macropores with size of 218 μm, with 20% absorbable fibers for additional porosity when the fibers degrade. hESCd-MSCs encapsulated in microbeads in CPC had good viability from 1 to 21 d. ALP gene expression at 21 d was 25-fold that at 1 d. Osteocalcin (OC) at 21 d was two orders of magnitude of that at 1 d. ALP activity in colorimetric *p*-nitrophenyl phosphate assay at 21 d was 5-fold that at 1 d. Mineral synthesis by the encapsulated hESCd-MSCs at 21 d was 7-fold that at 1 d. Potential benefits of the CPC-stem cell paste include injectability, intimate adaptation to complex-shaped bone defects, ease in contouring to achieve esthetics in maxillofacial repairs, and *in situ* setting ability. In conclusion, hESCd-MSCs were encapsulated in alginate microbeads in macroporous CPC showing good cell viability, osteogenic differentiation and mineral synthesis for the first time. The hESCd-MSC-encapsulating macroporous CPC construct is promising for bone regeneration in a wide range of orthopedic and maxillofacial applications.

*Correspondence: Hockin Xu, Professor, Director of Biomaterials & Tissue Engineering Division Department of Endodontics, Prosthodontics and Operative Dentistry, Dental School Center for Stem Cell Biology & Regenerative Medicine, School of Medicine University of Maryland, Baltimore, MD 21201 hxu@umaryland.edu Phone: 410-706-7047 Fax: 410-706-3028.

Keywords

Human embryonic stem cells; calcium phosphate cement; macroporosity; injectable scaffold; osteogenic differentiation; bone tissue engineering

1. Introduction

In 2004, the health care costs plus the lost wages for people in the United States with musculoskeletal diseases reached approximately $849 billion, or 7.7% of the national gross domestic product [1]. Skeletal diseases, congenital malformations, trauma, and post-cancer ablative surgery often require bone reconstruction, and the need is increasing dramatically as the population ages [2–6]. Tissue engineering approaches offer exciting promises to meet this need [7–12]. Extensive studies have resulted in significant progress in stem cell delivery via scaffolds with great potential for tissue regeneration [13–16].

Scaffolds are important for bone regeneration, and injectable scaffolds can be used in minimally-invasive procedures and fit intimately into complex-shaped defects [11,17–19]. Calcium phosphate (CaP) scaffolds mimic bone minerals, provide a more natural substrate for cell attachment and expression of osteoblast phenotype, and can bond to bone to form a functional interface [14,20–24]. For a preformed bioceramic to fit in a bone cavity, the surgeon needs to machine the graft or carve the surgical site, leading to increases in bone loss, trauma, and surgical time [17]. In contrast, calcium phosphate cements (CPC) are injectable and can self-harden *in situ* [19,25–29]. The first CPC was developed in 1986 [25] and approved in 1996 by the Food and Drug Administration (FDA) for repairing craniofacial defects [30]. Recent studies increased the macroporosity and mechanical strength of CPC by using porogens and absorbable fibers [31,32], and investigated stem cell seeding and ostegenic differentiation [33].

Besides scaffolds, stem cells are another key element in tissue engineering. Human bone marrow mesenchymal stem cells (hBMSCs) are frequently studied for bone engineering [2,3,6,9,10,34]. However, the harvest of hBMSCs requires an invasive procedure, and the hBMSC proliferation and differentiation potential is lost due to aging [35–37] and diseases, such as osteoporosis and arthritis [38,39]. With the baby boomers entering their senior years and with the prevalence of osteoporosis and arthritis, the very people who need bone repair are not able to provide potent hBMSCs for themselves. Therefore, there is a strong need for alternative stem cells for bone regeneration. Human embryonic stem cells (hESCs) are a highly promising cell source because of their potential for rapid proliferation to provide an unlimited supply of stem cells [16,40–45]. They have the capability to proliferate and self-renew over long periods of time and to differentiate into almost all cell types. For example, mesenchymal tissues could be formed by cells after long-term *in vitro* expansion till 63 population doublings [16]. However, there are only a few reports on the use of hESCs for bone engineering [16,41–48]. So far there has been no report on hESC seeding with CPC.

Osteoblasts and human umbilical cord MSCs were encapsulated into CPC [33,49,50]. The cells were first encapsulated into hydrogel microbeads, and the microbeads were then mixed with CPC to protect the cells from the CPC mixing and injection forces. The cells after injection had a good viability similar to that without injection [33]. The set CPC was biocompatible and the encapsulated cells were able to undergo osteogenic differentiation [33]. However, the encapsulation of hESCs and their osteogenic differentiation in CPC need to be investigated.

Accordingly, the objective of this study was to investigate CPC construct with alginate microbeads encapsulating hESCs for osteogenic differentiation for the first time. It was hypothesized that: (1) hESC-derived MSCs would remain viable while being encapsulated in alginate microbeads in macroporous CPC construct; (2) hESC-derived MSCs in microbeads in macroporous CPC construct could differentiate down the ostegenic lineage with elevated levels of alkaline phosphatase (ALP) and osteocalcin (OC) as well as bone mineral synthesis.

2. MATERIALS AND METHODS

2.1. hESC culture and propagation

hESCs were cultured to form three-dimensional cell aggregates called embryoid bodies (EBs), and the MSCs were then migrated out of the EBs [16,42]. hESCs (H9, Wicell, Madison, WI) usage was approved by the University of Maryland. The culture followed the Wicell protocol. Undifferentiated hESCs were cultured as colonies (an example in the present study is shown in Fig. 1A) on a feeder layer of mitotically-inactivated murine embryonic fibroblasts (MEF). The feeder layer had 200,000 MEF/well seeded on six-well culture plates (Nunclon Δ Surface, Nunc, Rochester, NY). Mitotic inactivation was achieved through exposure to 10 μg/mL Mitomycin C for 2 h. The medium consisted of 80% Dulbecco's modified Eagle medium (DMEM)/F12 (Invitrogen, Carlsbad, CA), 20% Knockout Serum Replacement (Invitrogen), 1 mM glutamine (Sigma, St. Louis, MO), 0.1 mM 2-Mercaptoethanol (Sigma), 1% modified Eagle medium (MEM) non-essential amino acids solution (Invitrogen) and 4 ng/mL basic fibroblast growth factor (β-FGF, Invitrogen). Cells were cultured at 37 °C with 5% CO_2 and 100% humidity, and the medium was changed daily. Cells were observed daily using a microscopy (TE2000-S, Nikon, Melville, NY). Colonies with differentiated morphologies were removed with fire-thrown Pasteur pipettes to ensure the undifferentiated expansion of hESCs. Passage of hESCs was achieved through mild enzymatic dissociation of colonies with 1 mg/mL collagenase type IV (Gibco, Gaithersburg, MD) for 5 min, followed by seeding on a fresh MEF layer.

2.2. hESC-derived MSCs

To simulate spontaneous differentiation, the hESCs were induced to form EBs [42,46]. Briefly, hESC colonies were dissociated into clumps through treatment with 1 mg/mL collagenase type IV for an extended duration of 10 min followed by scraping. The dissociated hESC clumps were transferred to 25 cm^2 ultra-low attachment culture flasks (Corning, Corning, NY) in EB formation medium, which consisted of DMEM (Invitrogen) supplemented with 20% fetal bovine serum (FBS) defined (Invitrogen), 1 mM glutamine (Sigma), 0.1 mM 2-Mercaptoethanol (Sigma), and 1% MEM non-essential amino acids solution (Invitrogen). The culture medium was changed every 2 d. Initially, the hESC clumps were largely composed of densely packed hESCs, creating simple EBs. After 4–5 d of suspension culture in the presence of an ultra-low attachment surface, the center of the bodies became cavitated and the bodies began to accumulate fluid and turn into free floating EBs (Fig. 1B). After 10 d, the EBs were transferred into six-well culture plates (Nunclon) and cultured for an additional 10 d, while the cells sprouted and migrated out of the EBs (Fig. 1C). Upon 70% confluence, the outgrowth cells were isolated by using cell scrapers and subcultured at an initial cell density of 2×10^4 cells/cm^2 in MSC growth medium. The MSC growth medium consisted of DMEM (Gibco) supplemented with 10% FBS (HyClone, Logan, UT), 2mM L-glutamine (Gibco), 100 U/mL penicillin, and 100 mg/mL streptomycin (Gibco) [42]. Examples of the differentiated cells thus obtained are shown in Fig. 1D. These cells expressed surface markers characteristic of MSCs, as shown below. These hESC-derived MSCs are referred to as hESCd-MSCs.

As an initial examination on whether the cells sprouted from the EBs were MSCs, the cells were cultured for 21 d in osteogenic medium, which consisted of the MSC growth medium supplemented with 50 μM ascorbic acid-2-phosphate, 10 mM β-glycerophosphate, 100 nM dexamethasone and 10 nM 1α,25-Dihydroxyvitamin (Sigma) [42]. Then the medium was discarded, and the cells were fixed with citrate-acetone-formaldehyde fixative for 45 seconds, and then stained with an ALP staining solution (Sigma) which stains ALP into a red color.

2.3. Flow cytometry of hESCd-MSCs

As a further examination on whether the cells sprouted from the EBs were MSCs, expression of the cell surface antigen profile was characterized using flow cytometry [42,46]. Passage 4 cells were harvested by trypsin-ethylenediaminetetraacetic acid (EDTA) and washed with cold phosphate buffered saline (PBS) containing 1% bovine serum albumin (BSA), then resuspended to approximately 1×10^6 cells in 50 μL of cold PBS containing 1% BSA. Cell samples were separately labeled on ice with optimal dilution of fluorescein isothiocyanate (FITC)-conjugated monoclonal antibodies (mAbs, from Invitrogen, unless otherwise noted) against CD29, CD31, CD34 (BD Pharmingen, San Jose, CA), CD44, CD45, CD73, TRA-1-81, HLA-ABC, and HLA-DR, phycoerythrin (PE)-conjugated mAbs against Oct3/4 and CD166, and Alexa Fluor 488 conjugated mAb against CD105 in the dark. After 30 min incubation, cells were washed with cold PBS. Nonspecific fluorescence was determined by incubating cells with isotype-matched conjugated mAbs. At least 10,000 events were collected from each run of flow cytometry. Data were analyzed using CellQuest software (Becton, San. Jose, CA). Fluorescence histogram for each mAb was displayed alongside the control antibody. The percentages of positive cells were subtracted from the isotype control antibody of each conjugate.

2.4. hESCd-MSC encapsulation in alginate microbeads

Alginate was used for cell encapsulation because it is non-cytotoxic and can form an ionically-crosslinked network under mild conditions without harming the cells. A 1.2% (mass) sodium alginate solution was prepared by dissolving alginate (Mw = 75,000 to 220,000 g/mol, ProNova, Norway) in a 155 mM sodium chloride solution [50]. hESCd-MSCs were encapsulated in alginate at a density of 1 million cells/mL [33]. Passage 4 cells were used for all experiments. The alginate-cell solution was loaded into a syringe connected to a bead-generating device (VarJ1, Nisco, Zurich, Switzerland). Sterile nitrogen gas was fed to the gas inlet and a pressure of 10 psi was established to form a coaxial air flow to break up the alginate droplets. The alginate droplets fell into a well of 100 mmol/L calcium chloride solution, where the alginate crosslinked and formed microbeads [33,50]. This method produced fine alginate microbeads with a mean diameter of 207 μm, suitable for injection application in CPC paste as shown in a previous study [33].

2.5. CPC powder, liquid, and mannitol porogen

CPC powder consisted of an equimolar mixture of tetracalcium phosphate ($Ca_4[PO_4]_2O$) and dicalcium phosphate anhydrous ($CaHPO_4$). Chitosan is biodegradable and osteoconductive, and can strengthen CPC and resist the washout of CPC paste in physiological solution [31]. Hence, CPC liquid consisted of chitosan malate (Halosource, Redmond, WA) mixed with water at a chitosan/(chitosan + water) of 15% by mass [31]. A degradable fiber (Vicryl, Ethicon, Somerville, NJ), a copolymer of glycolic and lactic acids, was cut into 3-mm filaments and mixed with CPC at a fiber volume fraction of 20% to reinforce the CPC [33]. In addition, a porogen was used to increase the porosity of CPC. Mannitol ($CH_2OH[CHOH]_4CH_2OH$, Sigma) was recrystallized in an ethanol/water solution at 50/50 by volume, and ground and sieved through openings of 125 μm (bottom sieve) and

250 μm (top sieve). The mannitol powder was mixed with the CPC powder at a mannitol/(CPC + mannitol) mass fraction of 30% [31].

2.6 Live/dead assay of encapsulated hECSd-MSCs

The CPC powder was mixed with chitosan liquid at (CPC power + fiber):liquid mass ratio of 2:1 to form a flowable paste, which was then mixed with the prescribed amount of mannitol porogen. First, 0.5 g of hESCd-MSC-encapsulating microbeads was placed at the bottom of each well of a 12-well plate. Then, 0.5 g of CPC composite paste was placed on top to cover the microbeads in each well. The CPC constructs were allowed to set at 37 °C for 30 min. Then, 3 mL of osteogenic medium was added to each well to submerge the construct. The medium was changed daily. After 1, 7, 14, and 21 d, the medium was removed, the CPC was carefully broken, and the hESCd-MSC-encapsulating microbeads were collected. Cells were live/dead stained for 30 min with 2 mL of PBS containing 2 μmol/L calcein-AM and 2 μmol/L ethidium homodimer-1 (Molecular Probes, Eugene, OR), and then observed using epifluorescence microscopy (Eclipse TE-2000S, Nikon). The percentage of live cells was measured as: $P = N_L / (N_L + N_D)$, where N_L was the number of live cells, and N_D was the number of dead cells [33]. The live cell density was measured as: $D = N_L/A$, where A was the area of the image where N_L was measured.

2.7. Osteogenic gene expressions of encapsulated hECSd-MSCs

ALP and OC gene expressions were measured via quantitative real-time reverse transcription polymerase chain reaction (qRT-PCR, 7900HT, Applied Biosystems, Foster City, CA). The total cellular RNA of the cells were extracted with TRIzol reagent (Invitrogen) and reverse-transcribed into cDNA using a High-Capacity cDNA Archive kit. TaqMan gene expression assay kits, including two pre-designed specific primers and probes, were used to measure the transcript levels of the proposed genes on human ALP (Hs00758162_m1), OC (Hs00609452_g1), and glyceraldehyde 3-phosphate dehydrogenase(GAPDH, Hs99999905). Relative expression for each target gene was evaluated using the $2^{-\Delta\Delta Ct}$ method [51]. C_t values of target genes were normalized by the C_t of the TaqMan human housekeeping gene GAPDH to obtain the ΔC_t values. The C_t value of hESC-MSCs cultured on tissue culture polystyrene in the control medium for 1 d served as the calibrator [33,52].

2.8. ALP protein activity of encapsulated hECSd-MSCs

ALP activity was measured using a colorimetric *p*-nitrophenyl phosphate (pNPP) assay (Stanbio, Boerne, TX) [13,14,24,33]. After culturing the constructs for 1, 7, 14, and 21 d, the culture medium was removed, the CPC was carefully broken, and the hESCd-MSC-encapsulating microbeads were collected. The microbeads were dissolved by 55 mmol/L sodium citrate tribasic solution (Sigma). A microplate reader (M5 SpectraMax, Molecular Devices, Sunnyvale, CA) was used and the ALP activity was normalized by the DNA content. DNA was quantified using a Quant-iT PicoGreen Kit (Invitrogen) [33,53].

2.9. Mineral synthesis by the encapsulated hESCd-MSCs

Minerals synthesized by cells in the microbeads in the constructs after 1, 7, 14 and 21 d in osteogenic medium were stained with xylenol orange. Xylenol orange is a fluorescent probe which chelates to calcium and stains mineral into a red color; it is not harmful to cells, and staining can be performed on live cells [54]. After 1, 7, 14, and 21 d, the CPC was carefully broken, and the hESCd-MSC-encapsulating microbeads were collected. Only the microbeads were stained, and the CPC matrix was not stained. The mineral area percentage was calculated as A_M/A, where A_M was the area of mineralization (red fluorescence), and A was the total area of the image [33]. The area of mineral for each image was computed using

NIS Elements imaging software (Nikon). In addition, two control groups were also examined: (1) Microbeads without cell encapsulation, which were placed in CPC construct for 1 d; (2) microbeads with cell encapsulation, which were cultured in tissue culture well for 1 d and were never encased in CPC. These microbeads were then collected for xylenol staining. The purpose of testing these controls was to eliminate the possibility that some CPC had leached into the hydrogels and was being picked up in xylenol staining. Six specimens were tested for each group (n = 6). Three randomly chosen fields of view were photographed from each specimen for a total of 18 photos for each condition.

2.10. CPC composite scaffold porosity

The CPC composite scaffolds were dried in a vacuum oven at 60 °C for 24 h. The dried specimens were placed in the chamber of a porosimeter (PoreMaster 33, Quantachrome, Boynton Beach, FL), which was then gradually filled with mercury up to a pressure of 210 MPa. The known chamber volume, mercury density and specimen weight enabled the specimen's volume, density and porosity to be calculated [31]. In addition, a scanning electron microscope (SEM, FEI Quanta 200, Hillsboro, OR) was used to examine the pore size and morphology in CPC specimens after being sputter-coated with gold.

One-way ANOVA was performed to detect significant effects of the variables. Tukey's multiple comparison tests were used at a p value of 0.05.

3. Results

Fig. 1 shows phase-contrast images of hESC culture. An example of a hESC colony was shown in (A) cultured on MEF feeder layer. Each hESC colony showed smooth edges that were distinctive from the feeder cells. When the colonies were dissociated into clumps, removed from MEF feeder and placed in suspension culture, the hESC clumps formed EBs, with an example shown in (B). During further culture, cells with a fibroblast-like morphology were observed to migrate out of the EBs (C). The outgrowth of cells sprouting from EBs attached to the culture plate. These cells became relatively uniform in size and shape after passage 3, with an example shown in (D). They had a similar morphology to fibroblasts and mesenchymal-like cells.

To examine if the cells migrated out of the EBs were MSCs (example in D), two tests were performed. First, the cells were cultured in growth medium or osteogenic medium for 21 d and then stained for ALP. In Fig. 1E, cells in growth medium had no ALP staining. In contrast, there was substantial ALP staining in the osteogenic medium in (F).

Second, flow cytometry analysis was performed (Fig. 2). MSC surface markers were consistently and highly expressed. The MSC surface markers CD29, CD44, CD73, and CD166 were expressed to levels > 99.4%. On the other hand, the expressions of hematopoietic markers (CD31, CD34, CD45) were less than 1.5%. Furthermore, HLA-ABC was expressed at 94.1%, whereas HLA-DR, TRA-1-81 and Oct3/4 were absent, which is characteristic for MSCs.

Fig. 3 shows the viability of the hESCd-MSCs encapsulated in microbeads in CPC. Typical live/dead images are shown in (A) and (B) at 1 d and 21 d, respectively. Live cells (green) were numerous, and dead cells (red) were few. The percentage of live cells is plotted in (C), which ranged from about 85% to 95%. The live cell density is plotted in (D), which is not significantly different from each other ($p > 0.1$). These results indicate that the encapsulated hESCd-MSCs maintained their viability and were not compromised in CPC from 1 to 21 d.

The osteogenic gene expressions are plotted in Fig. 4 for the encapsulated hESCd-MSCs in microbeads in CPC. In (A), the ALP expression was low at 1 d and 7 d, significantly ($p < 0.05$) increased at 14 d, and then greatly increased at 21 d. The ALP expression at 21 d was nearly 25-fold that at 1 d. In (B), the OC expression showed a similar trend. The OC expression at 21 d was two orders of magnitude that at 1 d.

The ALP activity measured via the colorimetric pNPP assay is plotted in Fig. 5. The DNA was measured (mean ± sd; n = 6) to be (29.6 ± 5.0) μg at 1 d, not significantly different from (24.0 ± 8.8) μg at 14 d, and (29.2 ± 6.4) μg at 21 d ($p > 0.1$). The ALP activity was low at 1 d, and significantly increased at 14 and 21 d ($p < 0.05$). These results indicate that the hESCd-MSCs encapsulated in alginate microbeads in the CPC construct successfully differentiated down the osteogenic lineage.

Fig. 6 shows results on mineral synthesis by the encapsulated hESC-MSCs in microbeads in CPC. Xylenol orange stains the minerals into a red color. The mineralization area was minimal at 1 d (A), and slightly increased at 7 d (B). There was much more mineral staining at 14 d and 21 d (C). The percentage of mineralization area is plotted in (D). The mineral synthesis by the encapsulated hESCd-MSCs at 21 d was 7-fold of that at 1 d. Representative xylenol staining images for the two controls are shown in (E) and (F). Microbeads retrieved from CPC construct without cells showed no red staining (F), indicating that the red staining in A–C was from the cells, and not from CPC. Microbeads with cells after 1 d in culture well without CPC had red staining similar to that after 1 d in CPC, indicating that placing the microbeads in CPC construct did not interfere with xylenol staining.

Since the porosity in CPC facilitates fluid circulation, the pores in CPC surfaces and cross-sections were examined via SEM. Fig. 7A shows typical macropores in CPC in the shapes of the entrapped mannitol particles. Examples of pore interconnection are shown in (B), where arrows indicate the open connections in the bottom of the macropore. The pore volume fraction of the CPC composite scaffold was measured (mean ± sd; n = 6) to be (64 ± 4)%. The macropore sizes ranged from approximately 50 to 343 μm, with an average pore size of 218 μm.

4. Discussion

The present study encapsulated hESCd-MSCs in alginate microbeads in macroporous CPC and investigated cell viability, osteogenic differentiation and mineral synthesis for the first time. A unique feature of this construct is its injectability. The present study focused on the study of hESCs, EBs and MSCs, without measuring the injectability of the composite paste. However, a previous study measured the injectability of the CPC composite paste with the same composition including the same-sized microbeads and the same amount of fibers [33]. Under an injection force of about 40 N, the entire paste was readily extruded through a 10-gauge needle similar to spinal needles used in the augmentation of osteoporotic vertebrae and the management of vertebral compression fractures. Measuring the percentage of live cells and the live cell density showed that the CPC mixing and injection process did not harm the encapsulated stem cells [33]. Hence, it is expected that the hESCd-MSCs in the CPC construct could potentially be injected in minimally invasive surgeries. The paste could also be placed into a bone cavity to yield intimate adaptation to complex-shaped defects with irregularities. The paste could be contoured and shaped for esthetics, especially in maxillofacial and cranial repairs, and then harden *in situ* with the encapsulated hESCd-MSCs to enhance bone regeneration.

Due to the exciting promise of hESCs for regenerative medicine applications, several studies were performed to investigate the use of hESCs for bone engineering [16,41–48]. Three-

dimensional poly(lactic-co-glycolic acid)/poly(L-lactic acid) polymer scaffold was used to support and promote hESC growth and differentiation, which showed promise for creating viable human tissue structures [40]. For cartilage tissue engineering, hESCs were cultured to yield EB-derived MSCs, and compressive mechanical stimulus enhanced the expression of cartilage-related markers [55]. For bone tissue engineering, osteogenic culture of hESCs yielded large quantities of functional osteogenic cells with bone matrix formation and mineralized collagen; cells were cultured on tissue culture plastic without a scaffold [41]. An *in vivo* study showed that ESC-derived construct implanted orthotopically in critical-sized cranial defects in rats successfully induced new bone formation; the cells were seeded on ceramic particles [44]. Another study described an efficient method of deriving MSCs from hESCs, by forming EBs first in suspension culture and then isolating the MSCs sprouting from the EBs [42], whose method the present study followed. EB-derived MSCs from human embryonic germ cells were differentiated to form mesenchymal tissues including bone, cartilage and adipose tissue, using cell-laden hydrogels [16]. Another study used poly(d,l-lactic-co-glycolic acid)/hydroxyapatite scaffolds seeded with hESC-derived osteogenic cells for bone regeneration in animals [43]. Collagen scaffolds were seeded with hESC-derived MSCs in immunocompromised mice, and these cells were capable of regenerating bone in calvarial defects [46]. In addition, nano-fibrous scaffold was used to seed hESCs for bone tissue engineering [47]. A recent study seeded hESC-derived osteogenic cells with hydroxyapatite/tricalcium phosphate ceramic powder and transplanted into immunocompromised mice showing an increased osteogenic potential [48]. While hESCs have the potential as an unlimited source of stem cells which are highly potent for regenerative medicine, only a small number of articles have been published on bone tissue engineering via hESCs [16,41–48]. These previous studies cultured the cells on tissue culture plates without a scaffold, or using ceramic particles, pre-fabricated polymer scaffolds, hydrogels, collagen, and nanofiber scaffolds. There has been no report on hESC encapsulation in CPC.

A difference between CPC and injectable polymers and hydrogels for cell encapsulation is the load-bearing capability. Previous studies reported that the strength was 0.7 MPa for injectable polymeric carriers for cell delivery [56], and 0.1 MPa for hydrogels [57,58]. The elastic modulus was 8 MPa for an injectable polymeric carrier [56], and 0.1 MPa for hydrogels [57,58]. These values are much lower than cancellous bone's strength of 3–10 MPa [59], and elastic modulus of about 300 MPa [60]. These injectable polymeric and hydrogel carriers are promising for tissue engineering in non-load-bearing locations. However, it was concluded that "Hydrogel scaffolds … do not possess the mechanical strength to be used in load bearing applications" [61]. Mechanical properties are of crucial importance for the regeneration of load-bearing tissues such as bone, to withstand stresses to avoid scaffold fracture, and to maintain the structure to define the shape of the regenerated tissue. In comparison, a previous study measured the mechanical properties of the injectable CPC containing the same amount of microbeads and fibers as the present study, and reported a flexural strength of 4 MPa and an elastic modulus of 680 GPa [33]. These values approximated the strength and modulus of cancellous bone. Hence, the injectable stem cell-encapsulating CPC construct is promising for a wide range of moderate load-bearing orthopedic applications.

hESCd-MSCs encapsulated in microbeads in CPC maintained a good viability from 1 to 21 d. The percentage of live cells ranged from 85% to 95%, consistent with previous studies on cell encapsulation [11,34,62]. The encapsulated cells did not proliferate and the live cell density was constant from 1 to 21 d. This is also consistent with previous studies showing that the encapsulated cells did not proliferate, which was because the cells were packed in hydrogel and were contact-inhibited, hence cell proliferation became arrested [34,63]. After mixing and placing the CPC paste, the set CPC is biocompatible and supports cell

attachment and differentiation [33]. Hence, after CPC has set, the microbeads could degrade inside CPC and release the cells to attach to CPC, while the microbead degradation could create additional macropores. The alginate microbeads in the present study showed little degradation in 21 d. It is desirable to use microbeads that can quickly degrade and release the cells after the CPC scaffold has set. Further study should investigate hESCd-MSC encapsulation in degradable microbeads, and examine cell release and proliferation inside the macroporous CPC.

hESCd-MSCs in microbeads in CPC were successfully differentiated into the osteogenic lineage, as confirmed by RT-PCR and ALP protein measurements as well as staining of mineral synthesis by the cells. The cells had high ALP and OC gene expressions, consistent with previous studies showing osteogenic differentiation of MSCs [52]. ALP and OC play important roles in the osteogenic differentiation of hESC-derived MSCs [16,41,42,46]. ALP is an enzyme expressed by MSCs during osteogenesis and is a well-defined marker for their differentiation [13,14,41,52,64]. Using hESC-derived MSCs, the ALP of cells cultured in osteogenic medium was 3–6 fold of the ALP without osteogenic supplements [41]. Another study on hESC-derived MSCs showed that the differentiated cells had an ALP about 15-fold of the ALP of undifferentiated cells [41]. Using human embryonic germ derived cells, the ALP for differentiated cells was about 10-fold that for undifferentiated cells, the OC was also increased by 10-fold for differentiated cells [16]. The osteogenic differentiation and mineralization were shown at 14 to 21 d [16]. These results are consistent with the present study on hESCd-MSCs, which showed that both ALP and OC gene expressions were increased by 10–100 folds at 14 and 21 d, ALP activity at 21 d was 5-fold of the ALP at 1 d, and mineralization at 21 d was 7-fold of that at 1 d. These results together demonstrate that the encapsulated hESCd-MSCs in the CPC construct differentiated down the osteogenic lineage and synthesized bone minerals. While hESCs are promising for bone regeneration and serve as an alternative to autologous transplant especially for patients whose autologous MSCs are not sufficient or potent, immune rejection remains a challenge. One potential strategy to overcome the immunological rejection is to create stem cell banks comprising of HLA-typed hESCs by providing HLA-matched (histocompatible) tissue for the target population [65]. Further research is needed to address the immunological issues of hESCs.

The CPC composite scaffold had a porosity of 64%, with an average macropore size of 218 μm. Previous studies reported that macropores of sizes of several hundred microns were suitable for cell migration and tissue ingrowth [21]. The interconnected porosity helped provide access to culture medium and contributed to the cell viability. CPC has an intrinsic porosity of about 30–40% consisting of micron-sized micropores, due to the mixing of CPC powder with a liquid containing water. However, without additional macropores, the intrinsic CPC porosity was insufficient to provide the encapsulated cells with access to culture medium. This was shown in a recent study, in which the percentage of live cells was only about 50% inside CPC without macropores, and increased to 85% with the creation of macropores in CPC [66]. The porosity of 64% for the CPC scaffold exceeded the reported 40% of porosity for a hydroxyapatite scaffold in a previous study [21]. In addition, it should be mentioned that the CPC contained 20% of absorbable fibers with a diameter of 322 μm and a length of 3 mm (3000 μm). These fibers could provide reinforcement for several weeks, and then degrade and create additional cylindrical macropores in CPC [31]. The porosity and pore interconnection of the CPC of the present study would be useful to enable the circulation of physiological fluids and nutrients to enhance cell function. In addition, CPC was resorbable and was replaced by new bone after 6 months [67] to 18 months [30]. CPC showed excellent soft tissue response, and demonstrated steadfast adherence to the adjacent bone [68]. After 6 months, 12% to 25% by volume of CPC was resorbed *in vivo* [68]. After the scaffold was implanted *in vivo*, the mechanical strength of the scaffold increased over time when new bone started to grow into the macropores [69]. Therefore, it is

in the early stage of implantation when the macroporous implant is in the most need of strength. Hence, the rationale of the absorbable fibers in CPC was to provide the needed early strength, and then after significant new bone formation *in vivo*, the fibers would degrade and create additional macropores for continued tissue ingrowth. The creation of these macropores in CPC, along with the observed good viability of the hESCd-MSCs, the highly elevated ALP and OC and the synthesis of bone mineral, suggest the potential of this novel construct for bone regeneration. Further study is needed to investigate bone formation in an animal model via hESCd-MSCs delivered in an injectable and macroporous CPC scaffold.

5. Conclusion

The present study developed hESCd-MSC-encapsulating hydrogel microbeads in macroporous CPC construct and investigated osteogenic differentiation and mineral synthesis for the first time. The cells that sprouted from the EBs showed surface markers characteristic for MSCs. The encapsulated hESCd-MSCs maintained a good viability in the construct from 1 d to 21 d. The ALP and OC gene expressions for the encapsulated hESCd-MSCs were increased by 10–100 folds at 14 and 21 d. ALP activity at 21 d was 5-fold of the ALP at 1 d, and mineralization at 21 d was 7-fold of that at 1 d. These results demonstrate that the encapsulated hESCd-MSCs in the macroporous CPC construct differentiated down the osteogenic lineage and synthesized bone minerals. The CPC scaffold had a porosity of 64% and macropore size of 218 μm, which contributed to culture medium access and cell viability. Potential benefits of the CPC-stem cell paste include its injectability, intimate adaptation to irregularly-shaped bone defects, ease in contouring to achieve esthetics in maxillofacial repairs, and *in situ* setting capability. hESCs are exciting because of their ability for rapid proliferation to provide an unlimited supply of stem cells, and this study showed that these cells are suitable for delivery and differentiation in CPC. The hESCd-MSC-encapsulating macroporous CPC construct is promising for bone regeneration in a wide range of orthopedic and maxillofacial applications.

Acknowledgments

We are indebted to Dr. Ferenc Livak for help with flow cytometry which were performed at the University of Maryland Greenbaum Cancer Center Shared Flow Cytometry Facility. We also thank Dr. Larry C. Chow, Dr. Shozo Takagi, and Dr. Carl G. Simon for helpful discussions. This study was supported by NIH R01 DE14190 and DE17974 (HX), Maryland Stem Cell Fund (HX), and the University of Maryland School of Dentistry.

References

1. United States Bone and Joint Decade (USBJD) 2002–2011. Rosemont, IL: American Academy of Orthopaedic Surgeons; 2008. The Burden of Musculoskeletal Diseases in the United States. Forward.
2. Salgado AJ, Coutinho OP, Reis RL. Bone tissue engineering: state of the art and future trends. Macromol Biosci. 2004; 4:743–765. [PubMed: 15468269]
3. Mikos AG, Herring SW, Ochareon P, Elisseeff J, Lu HH, Kandel R, et al. Engineering complex tissues. Tissue Eng. 2006; 12:3307–3339. [PubMed: 17518671]
4. Ginebra MP, Traykova T, Planell JA. Calcium phosphate cements as bone drug-delivery systems: a review. J Controlled Release. 2006; 113:102–110.
5. Russias J, Saiz E, Deville S, Gryn K, Liu G, Tomsia AP. Fabrication and *in vitro* characterization of three-dimensional organic/inorganic scaffolds by robocasting. J Biomed Mater Res A. 2007; 83:434–445. [PubMed: 17465019]
6. Mao, JJ.; Vunjak-Novakovic, G.; Mikos, AG.; Atala, A. Regenerative medicine: Translational approaches and tissue engineering. Boston, MA: Artech House; 2007.

7. Lavik E, Langer R. Tissue engineering: Current state and perspectives. Applied Microbiol & Biotech. 2004; 65:1–8.
8. Hill EE, Boontheekul T, Mooney DJ. Regulating activation of transplanted cells controls tissue regeneration. Proc Natl Acad Sci USA. 2006; 103:2494–2499. [PubMed: 16477029]
9. Mao JJ, Giannobile WV, Helms JA, Hollister SJ, Krebsbach PH, Longaker MT, et al. Craniofacial tissue engineering by stem cells. J Dent Res. 2006; 85:966–979. [PubMed: 17062735]
10. Johnson PC, Mikos AG, Fisher JP, Jansen JA. Strategic directions in tissue engineering. Tissue Eng. 2007; 13:2827–2837. [PubMed: 18052823]
11. Salinas CN, Anseth KS. The influence of the RGD peptide motif and its contextual presentation in PEG gels on human mesenchymal stem cell viability. J Tissue Eng Regen Med. 2008; 2:296–304. [PubMed: 18512265]
12. Atala A. Engineering organs. Curr Opin Biotechnol. 2009; 20:575–592. [PubMed: 19896823]
13. Benoit DSW, Nuttelman CR, Collins SD, Anseth KS. Synthesis and characterization of a fluvastatin-releasing hydrogel delivery system to modulate hMSC differentiation and function for bone regeneration. Biomaterials. 2006; 27:6102–6110. [PubMed: 16860387]
14. Reilly GC, Radin S, Chen AT, Ducheyne P. Differential alkaline phosphatase responses of rat and human bone marrow derived mesenchymal stem cells to 45S5 bioactive glass. Biomaterials. 2007; 28:4091–4097. [PubMed: 17586040]
15. Sundelacruz S, Kaplan DL. Stem cell- and scaffold-based tissue engineering approaches to osteochondral regenerative medicine. Semin Cell Dev Biol. 2009; 20:646–655. [PubMed: 19508851]
16. Varghese S, Hwang NS, Ferran A, Hillel A, Theprungsirikul P, Canver AC, et al. Engineering musculoskeletal tissues with human embryonic germ cell derivatives. Stem Cells. 2010; 28:765–774. [PubMed: 20178108]
17. Laurencin CT, Ambrosio AMA, Borden MD, Cooper JA. Tissue engineering: Orthopedic applications. Annual Rev Biomed Eng. 1999; 1:19–46. [PubMed: 11701481]
18. Gomes, ME.; Mikos, AG.; Reis, RL. Injectable polymeric scaffolds for bone tissue engineering. In: Reis, RL.; San Roman, J., editors. Biodegradable Systems in Tissue Engineering and Regenerative Medicine. Boca Raton, FL: CRC Press; 2004. p. 29-38.
19. Bohner M. Design of ceramic-based cements and putties for bone graft substitution. Eur Cell Mater. 2010; 20:1–12. [PubMed: 20574942]
20. Ducheyne P, Qiu Q. Bioactive ceramics: The effect of surface reactivity on bone formation and bone cell function. Biomaterials. 1999; 20:2287–2303. [PubMed: 10614935]
21. Pilliar RM, Filiaggi MJ, Wells JD, Grynpas MD, Kandel RA. Porous calcium polyphosphate scaffolds for bone substitute applications -*in vitro* characterization. Biomaterials. 2001; 22:963–972. [PubMed: 11311015]
22. Foppiano S, Marshall SJ, Marshall GW, Saiz E, Tomsia AP. The influence of novel bioactive glasses on in vitro osteoblast behavior. J Biomed Mater Res A. 2004; 71:242–249. [PubMed: 15372470]
23. Deville S, Saiz E, Nalla RK, Tomsia AP. Freezing as a path to build complex composites. Science. 2006; 311:515–518. [PubMed: 16439659]
24. Leach JK, Kaigler D, Wang Z, Krebsbach PH, Mooney DJ. Coating of VEGF-releasing scaffolds with bioactive glass for angiogenesis and bone regeneration. Biomaterials. 2006; 27:3249–3255. [PubMed: 16490250]
25. Brown, WE.; Chow, LC. A new calcium phosphate water setting cement. In: Brown, PW., editor. Cements Research Progress. Westerville, OH: American Ceramics Society; 1986. p. 352-379.
26. Barralet JE, Gaunt T, Wright AJ, Gibson IR, Knowles JC. Effect of porosity reduction by compaction on compressive strength and microstructure of calcium phosphate cement. J Biomed Mater Res B. 2002; 63:1–9.
27. Ginebra MP, Driessens FC, Planell JA. Effect of the particle size on the micro and nanostructural features of a calcium phosphate cement: a kinetic analysis. Biomaterials. 2004; 25:3453–3462. [PubMed: 15020119]
28. Bohner M, Baroud G. Injectability of calcium phosphate pastes. Biomaterials. 2005; 26:1553–1563. [PubMed: 15522757]

29. Bodde EW, Habraken WJ, Mikos AG, Spauwen PH, Jansen JA. Effect of polymer molecular weight on the bone biological activity of biodegradable polymer/calcium phosphate cement composites. Tissue Eng A. 2009; 15:3183–3191.

30. Friedman CD, Costantino PD, Takagi S, Chow LC. BoneSource hydroxyapatite cement: a novel biomaterial for craniofacial skeletal tissue engineering and reconstruction. J Biomed Mater Res B. 1998; 43:428–432.

31. Xu HHK, Takagi S, Quinn JB, Chow LC. Fast-setting and anti-washout calcium phosphate scaffolds with high strength and controlled macropore formation rates. J Biomed Mater Res A. 2004; 68:725–734. [PubMed: 14986327]

32. Xu HHK, Weir MD, Burguera EF, Fraser AM. Injectable and macroporous calcium phosphate cement scaffold. Biomaterials. 2006; 27:4279–4287. [PubMed: 16650891]

33. Zhao L, Weir MD, Xu HHK. An injectable calcium phosphate - alginate hydrogel - umbilical cord mesenchymal stem cell paste for bone tissue engineering. Biomaterials. 2010; 31:6502–6510. [PubMed: 20570346]

34. Nuttelman CR, Tripodi MC, Anseth KS. *In vitro* osteogenic differentiation of human mesenchymal stem cells photoencapsulated in PEG hydrogels. J Biomed Mater Res A. 2004; 68:773–782. [PubMed: 14986332]

35. Mueller SM, Glowacki J. Age-related decline in the osteogenic potential of human bone marrow cells cultured in three-dimensional collagen sponges. J Cell Biochem. 2001; 82:583–590. [PubMed: 11500936]

36. Mendes SC, Tibbe JM, Veenhof M, Bakker K, Both S, Platenburg PP, et al. Bone tissue-engineered implants using human bone marrow stromal cells: Effect of culture conditions and donor age. Tissue Eng. 2002; 8:911–920. [PubMed: 12542937]

37. Stenderup K, Justesen J, Clausen C, Kassem M. Aging is associated with decreased maximal life span and accelerated senescence of bone marrow stromal cells. Bone. 2003; 33:919–926. [PubMed: 14678851]

38. Rodriguez JP, Montecinos L, Rios S, Reyes P, Martinez J. Mesenchymal stem cells from osteoporotic patients produce a type I collagen-deficient extracellular matrix favoring adipogenic differentiation. J Cell Biochem. 2000; 79:557–565. [PubMed: 10996846]

39. Suzuki Y, Kim KJ, Kotake S, Itoh T. Stromal cell activity in bone marrow from the tibia and iliac crest of patients with rheumatoid arthritis. J Bone Miner Metab. 2001; 19:56–60. [PubMed: 11156475]

40. Levenberg S, Huang NF, Lavik E, Rogers AB, Itskovitz-Eldor J, Langer R. Differentiation of human embryonic stem cells on three-dimensional polymer scaffolds. Proc Natl Acad Sci USA. 2003; 100:12741–12746. [PubMed: 14561891]

41. Karp JM, Ferreira LS, Khademhosseini A, Kwon AH, Yeh J, Langer RS. Cultivation of human embryonic stem cells without the embryoid body step enhances osteogenesis in vitro. Stem Cells. 2006; 24:835–843. [PubMed: 16253980]

42. Hwang NS, Varghese S, Lee HJ, Zhang Z, Ye Z, Bae J, et al. *In vivo* commitment and functional tissue regeneration using human embryonic stem cell-derived mesenchymal cells. Proc Natl Acad Sci USA. 2008; 105:20641–20646. [PubMed: 19095799]

43. Kim S, Kim SS, Lee SH, Eun AS, Gwak SJ, Song JH, et al. *In vivo* bone formation from human embryonic stem cell-derived osteogenic cells in poly(D,L-lactic-co-glycolic acid)/hydroxyapatite composite scaffolds. Biomaterials. 2008; 29:1043–1053. [PubMed: 18023477]

44. Jukes JM, Both SK, Leusink A, Sterk LM, van BCA, de Boer J. Endochondral bone tissue engineering using embryonic stem cells. Proc Natl Acad Sci USA. 2008; 105:6840–6845. [PubMed: 18467492]

45. Jukes JM, Both SK, van BCA, de Boer J. Potential of embryonic stem cells for in vivo bone regeneration. Regen Med. 2008; 3:783–785. [PubMed: 18947301]

46. Arpornmaeklong P, Brown SE, Wang Z, Krebsbach PH. Phenotypic characterization, osteoblastic differentiation, and bone regeneration capacity of human embryonic stem cell-derived mesenchymal stem cells. Stem Cells Dev. 2009; 18:955–968. [PubMed: 19327009]

47. Smith LA, Liu X, Hu J, Ma PX. The enhancement of human embryonic stem cell osteogenic differentiation with nano-fibrous scaffolding. Biomaterials. 2010; 31:5526–5535. [PubMed: 20430439]
48. Kuznetsov SA, Cherman N, Robey PG. *In vivo* bone formation by progeny of human embryonic stem cells. Stem Cells Dev. 2011; 20:269–287. [PubMed: 20590404]
49. Simon CG Jr, Guthrie WF, Wang FW. Cell seeding into calcium phosphate cement. J Biomed Mater Res A. 2004; 68:628–639. [PubMed: 14986318]
50. Weir MD, Xu HHK, Simon CG Jr. Strong calcium phosphate cement-chitosan-mesh construct containing cell-encapsulating hydrogel beads for bone tissue engineering. J Biomed Mater Res A. 2006; 77:487–496. [PubMed: 16482548]
51. Livak KJ, Schmittgen TD. Analysis of relative gene expression data using real-time quantitative PCR and the $2^{-\Delta\Delta Ct}$ method. Methods. 2001; 25:402–408. [PubMed: 11846609]
52. Kim K, Dean D, Mikos AG, Fisher JP. Effect of initial cell seeding density on early osteogenic signal expression of rat bone marrow stromal cells cultured on cross-linked poly(propylene fumarate) disks. Biomacromolecules. 2009; 10:1810–1817. [PubMed: 19469498]
53. Weir MD, Xu HHK. Osteoblastic induction on calcium phosphate cement-chitosan constructs for bone tissue. J Biomed Mater Res A. 2010; 94:223–233. [PubMed: 20166217]
54. Wang YH, Liu Y, Maye P, Rowe DW. Examination of mineralized nodule formation in living osteoblastic cultures using fluorescent dyes. Biotechnol Prog. 2006; 22:1697–1701. [PubMed: 17137320]
55. Terraciano V, Hwang N, Moroni L, Park HB, Zhang Z, Mizrahi J, et al. Differential response of adult and embryonic mesenchymal progenitor cells to mechanical compression in hydrogels. Stem Cells. 2007; 25:2730–2738. [PubMed: 17702983]
56. Shi X, Sitharaman B, Pham QP, Liang F, Wu K, Billups WE, et al. Fabrication of porous ultra-short single-walled carbon nanotube nanocomposite scaffolds for bone tissue engineering. Biomaterials. 2007; 28:4078–4090. [PubMed: 17576009]
57. Drury JL, Dennis RG, Mooney DJ. The tensile properties of alginate hydrogels. Biomaterials. 2004; 25:3187–3199. [PubMed: 14980414]
58. Kuo CK, Ma PX. Ionically crosslinked alginate hydrogels as scaffolds for tissue engineering: Part I. Structure, gelation rate and mechanical properties. Biomaterials. 2001; 22:511–521. [PubMed: 11219714]
59. Christiansen BA, Kopperdahl DL, Kiel DP, Keaveny TM, Bouxsein ML. Mechanical contributions of the cortical and trabecular compartments contribute to differences in age-related changes in vertebral body strength in men and women assessed by QCT-based finite element analysis. J Bone Miner Res. 2011; 26:974–983. [PubMed: 21542000]
60. O'Kelly K, Tancred D, McCormack B, Carr A. A quantitative technique for comparing synthetic porous hydroxyapatite structure and cancellous bone. J Mater Sci: Mater in Med. 1996; 7:207–213.
61. Drury JL, Mooney DJ. Review. Hydrogels for tissue engineering: scaffold design variables and applications. Biomaterials. 2003; 24:4337–4351. [PubMed: 12922147]
62. Kong HJ, Smith MK, Mooney DJ. Designing alginate hydrogels to maintain viability of immobilized cells. Biomaterials. 2003; 24:4023–4029. [PubMed: 12834597]
63. Markusen JF, Mason C, Hull DA, Town MA, Tabor AB, Clements M, et al. Behavior of adult human mesenchymal stem cells entrapped in alginate-GRGDY beads. Tissue Eng. 2006; 12:821–830. [PubMed: 16674295]
64. Hofmann S, Hagenmuller H, Koch AM, Muller R, Vunjak-Novakovic G, Kaplan DL, et al. Control of in vitro tissue-engineered bone-like structures using human mesenchymal stem cells and porous silk scaffolds. Biomaterials. 2007; 28:1152–1162. [PubMed: 17092555]
65. Taylor CJ, Bolton EM, Bradley JA. Immunological considerations for embryonic and induced pluripotent stem cell banking. Philos Trans R Soc Lond B Biol Sci. 2011; 366:2312–2322. [PubMed: 21727137]
66. Chen W, Zhou H, Tang M, Weir MD, Bao C, Xu HHK. Macroporous gas-foaming calcium phosphate cement encapsulation of human umbilical cord stem cells. Tissue Engineering A. 2011 accepted for publication.

67. Sugawara A, Fujikawa K, Kusama K, Nishiyama M, Murai S, Takagi S, Chow LC. Histopathologic reaction of a calcium phosphate cement for alveolar ridge augmentation. J Biomed Mater Res. 2002; 61:47–52. [PubMed: 12001245]

68. Stelnicki EJ, Ousterhout DK. Hydroxyapatite paste (Bone Source) used as an onlay implant for supraorbital and malar augmentation. J Craniofacial Surgery. 1997; 8:367–372.

69. Martin RB, Chapman MW, Holmes RE, Sartoris DJ, Shors EC, Gordon JE, et al. Effects of bone ingrowth on the strength and non-invasive assessment of a coralline hydroxyapatite material. Biomaterials. 1989; 10:481–488. [PubMed: 2804236]

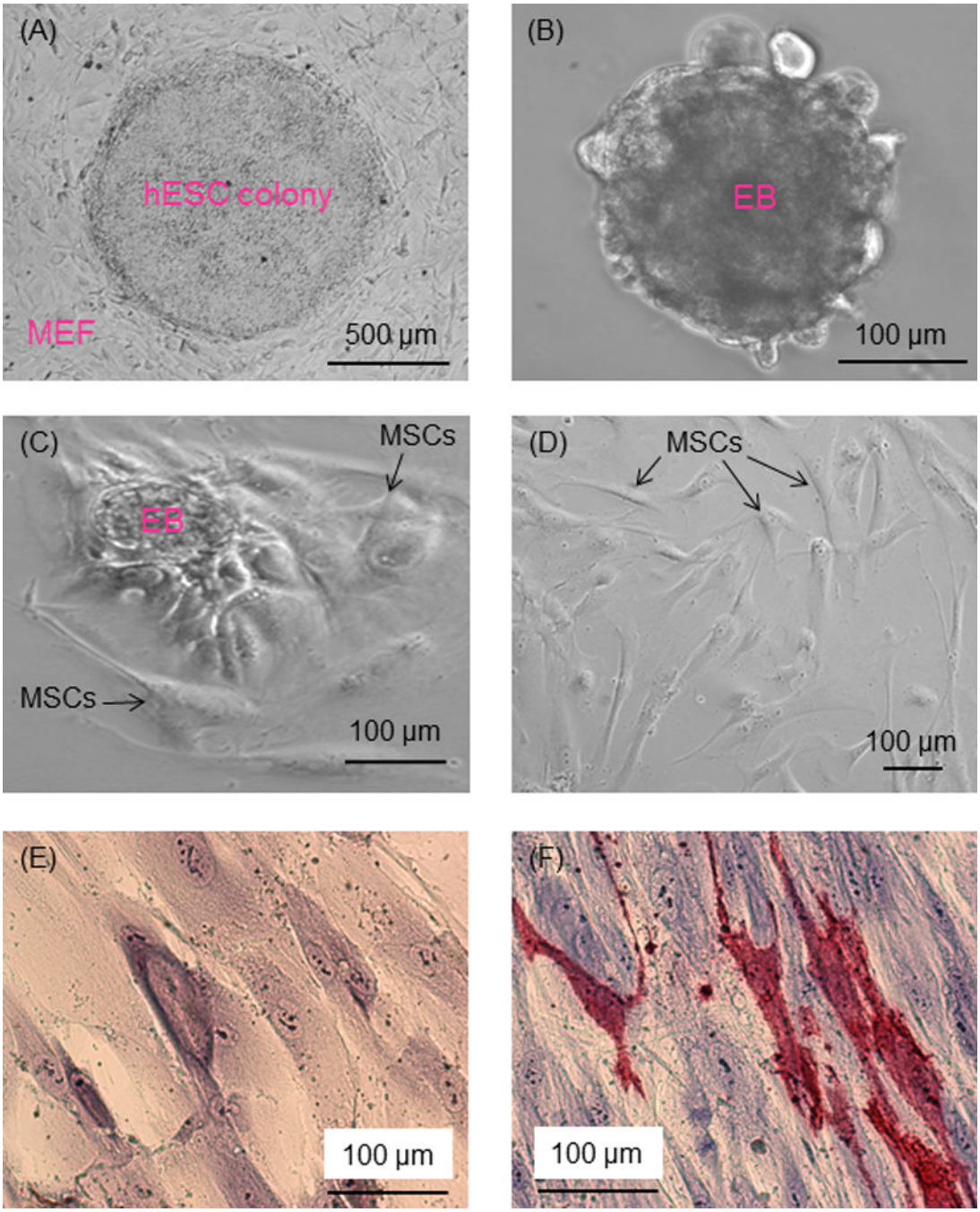

Figure 1.

Phase-contrast images of hESC culture. (A) hESC colonies were cultured on MEF feeder layer. (B) hESC colonies were dissociated into clumps, which formed EBs in suspension culture. (C) In further culture of EBs, cells migrated out of the EBs. (D) The outgrowth of cells had a morphology similar to MSCs (passage 3 shown in the example in D). (E, F) Passage 4 cells were cultured in MSC growth medium or osteogenic medium for 21 d. Cells in growth medium had no ALP staining (E). Cells in osteogenic medium had ALP staining (F), where red color represents ALP-positive cells.

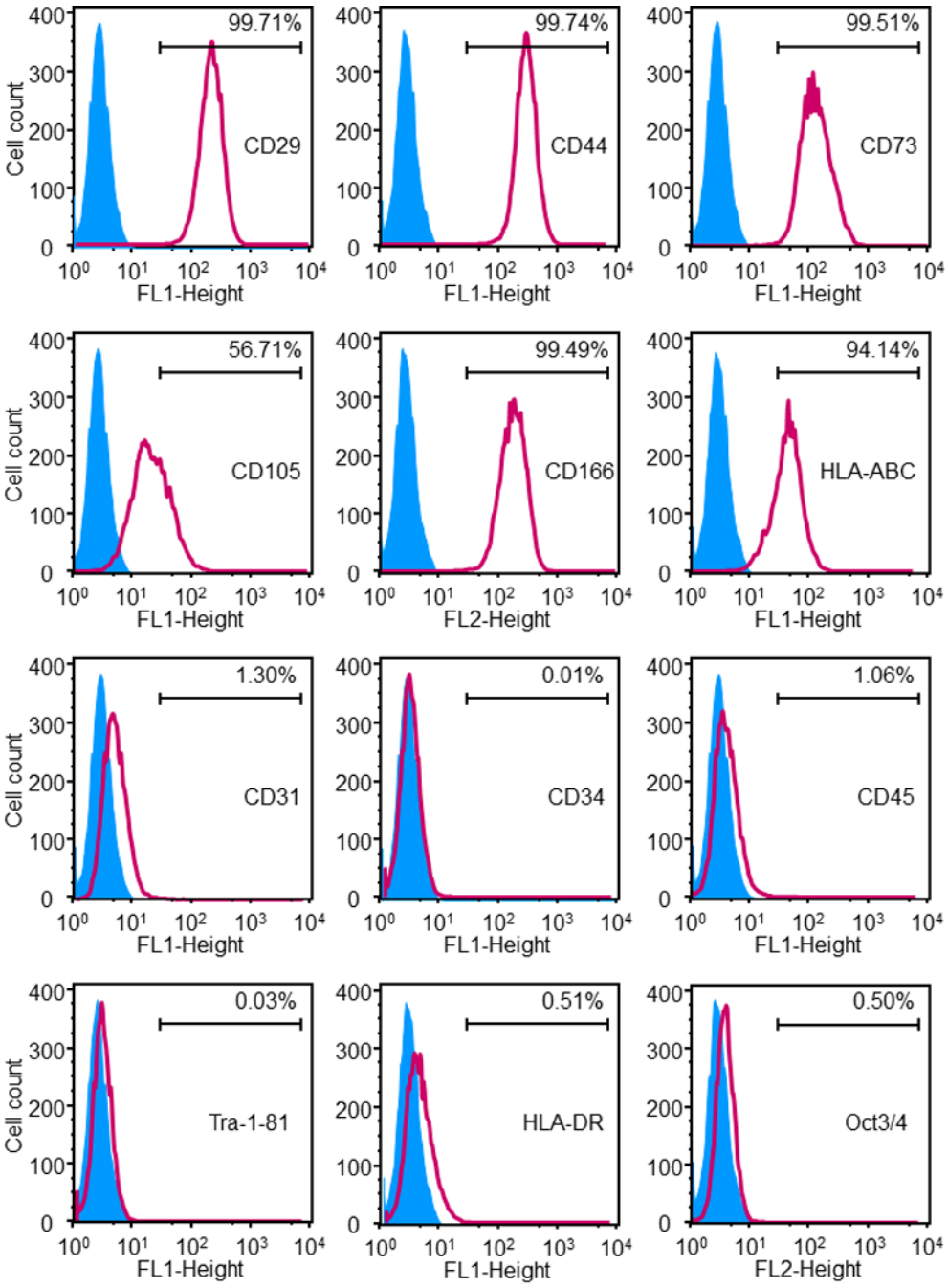

Figure 2.

Immunophenotyping of the hESCd-MSCs. Flow cytometry showed that hESCd-MSCs expressed a number of cell surface markers characteristic of MSCs, and were negative for typical hematopoietic and endothelial cell markers. For example, MSC surface markers CD29, CD44, CD73, and CD166 were expressed to levels greater than 99.4%, while expressions of hematopoietic markers (CD31, CD34, CD45) were less than 1.5%.

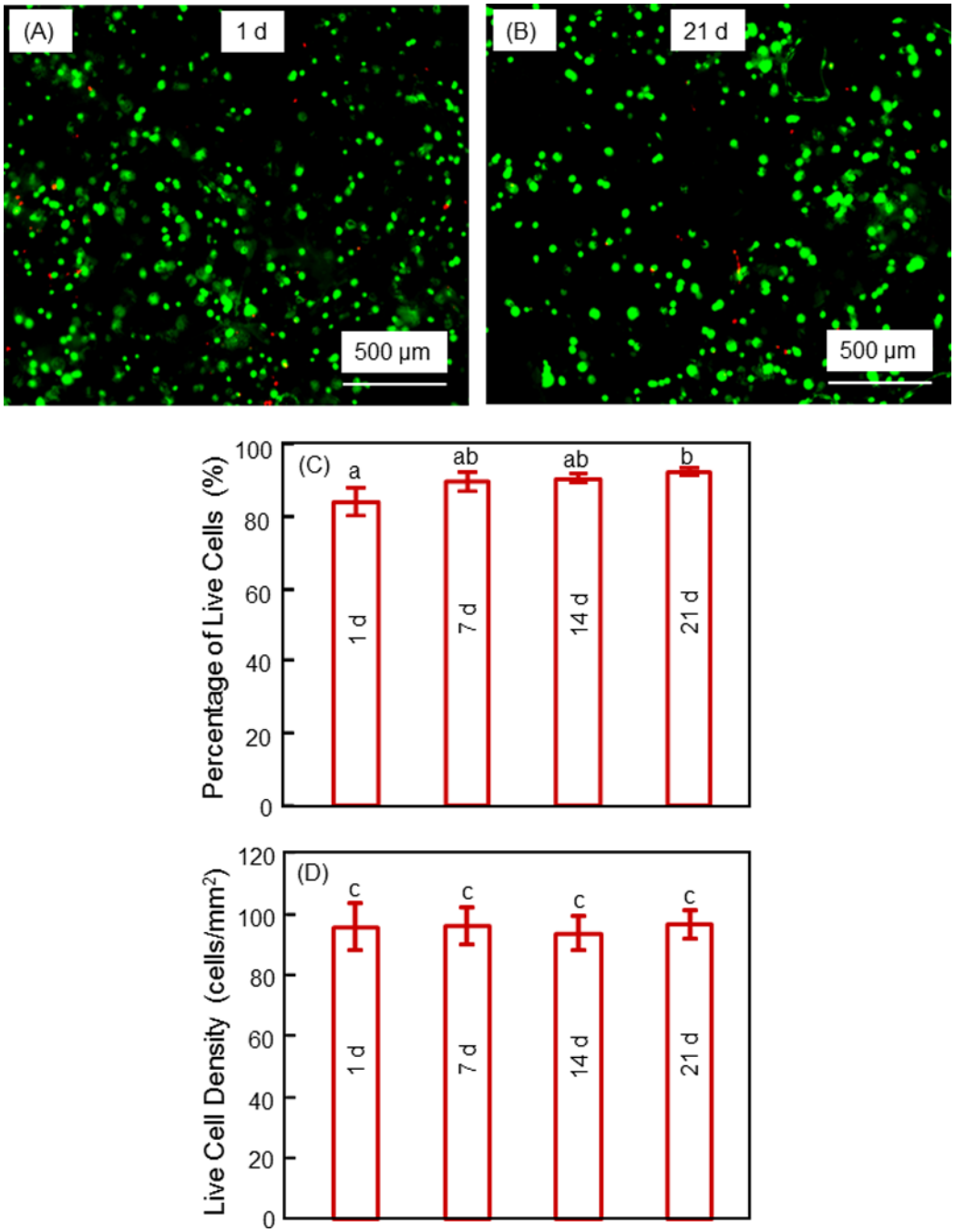

Figure 3.

Viability of hESCd-MSCs encapsulated in alginate microbeads in CPC construct. (A, B) Typical live/dead images at 1 d and 21 d, respectively. Live cells (green) were numerous, and dead cells (red) were few. (C) Percentage of live cells. (D) Live cell density. Each value is mean ± sd (n = 6). Values with dissimilar letters are significantly different from each other ($p < 0.05$). These results indicate that the encapsulated hESCd-MSCs maintained their viability from 1 to 21 d.

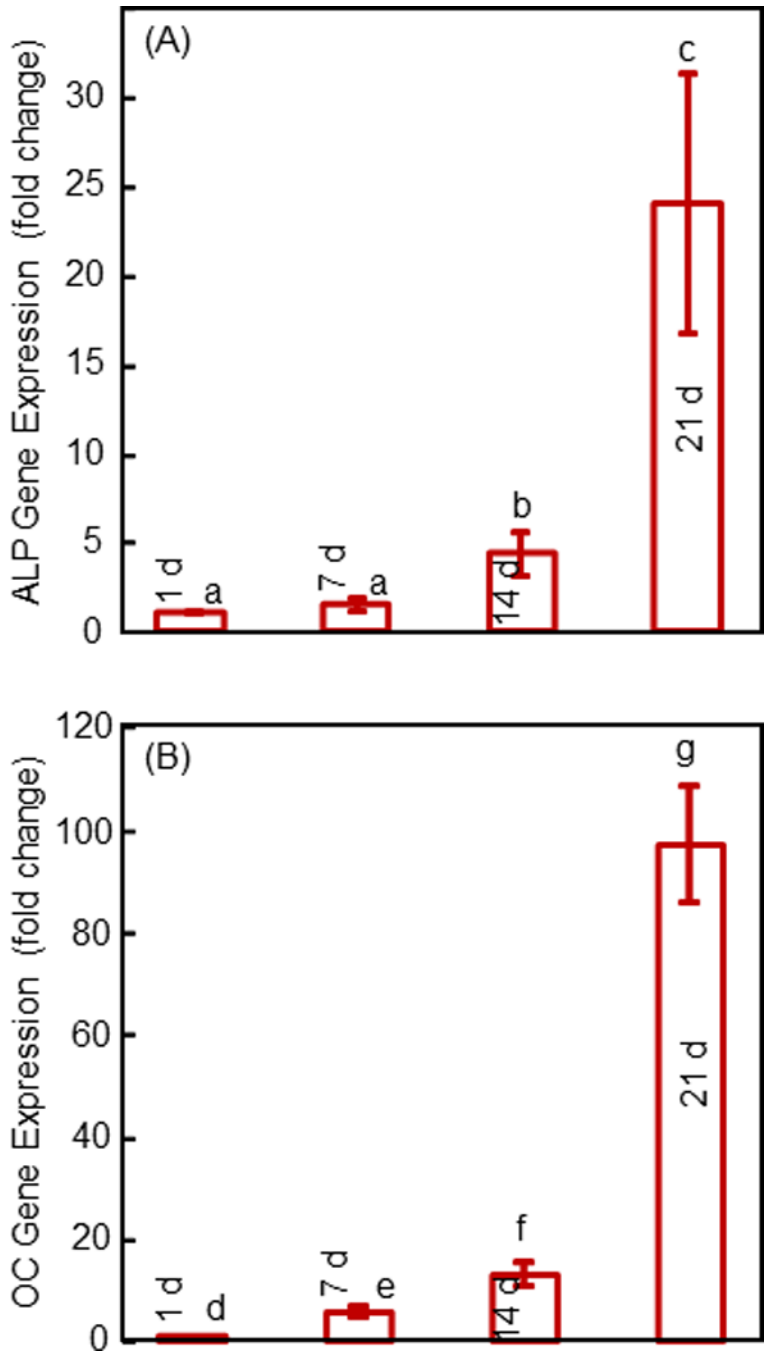

Figure 4.

Osteogenic gene expression of hESCd-MSCs in alginate microbeads in CPC measured by RT-PCR: (A) Alkaline phosphatase (ALP), and (B) osteocalcin (OC) gene expressions. Each value is mean ± sd (n = 6). Values with dissimilar letters are different from each other ($p < 0.05$).

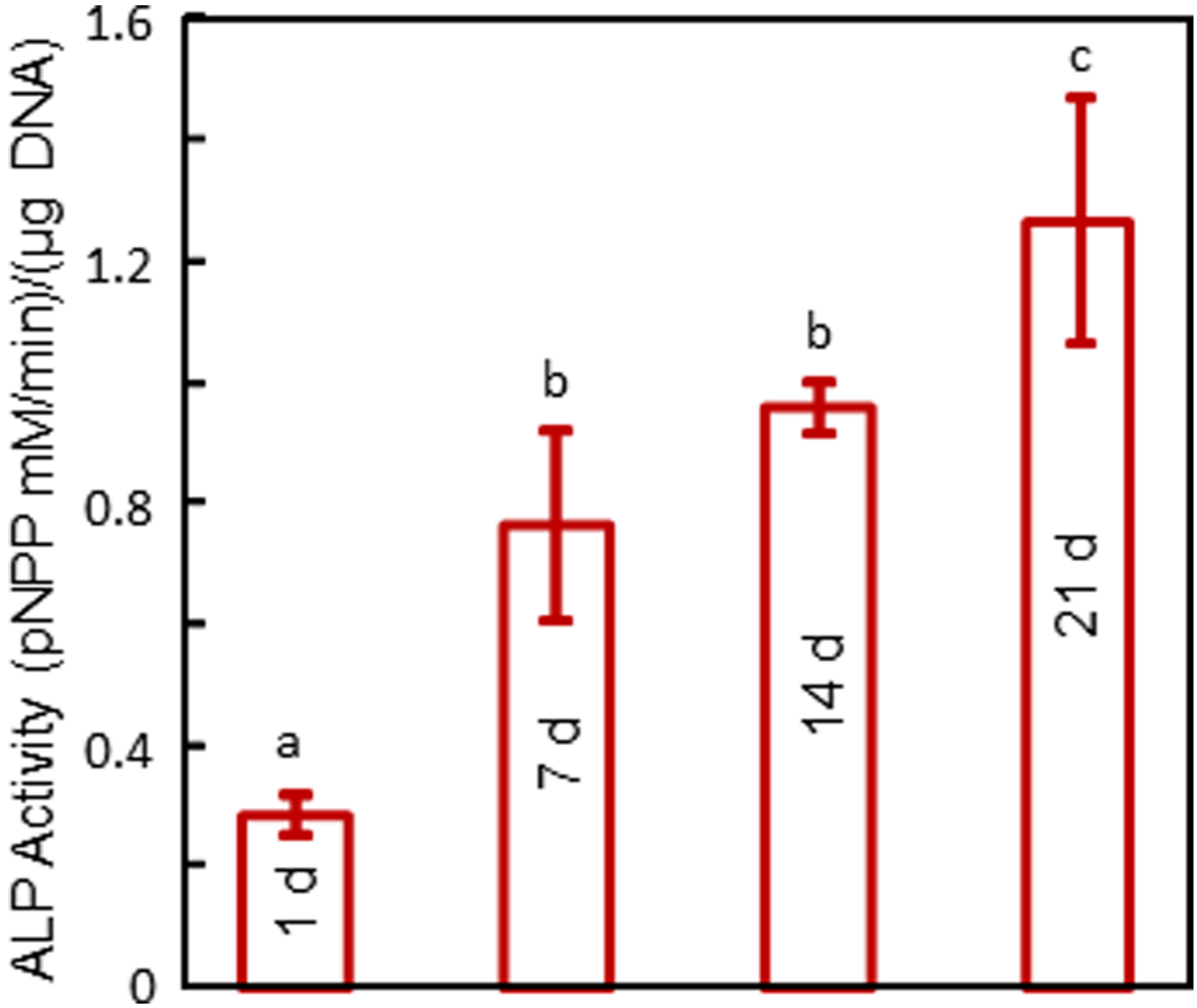

Figure 5.
ALP activity of hESCd-MSCs in alginate microbeads in CPC measured via a colorimetric pNPP assay. Each value is mean ± sd (n = 6). Values with dissimilar letters are different from each other ($p < 0.05$). These results indicate that the encapsulated hESCd-MSCs successfully differentiated down the osteogenic lineage.

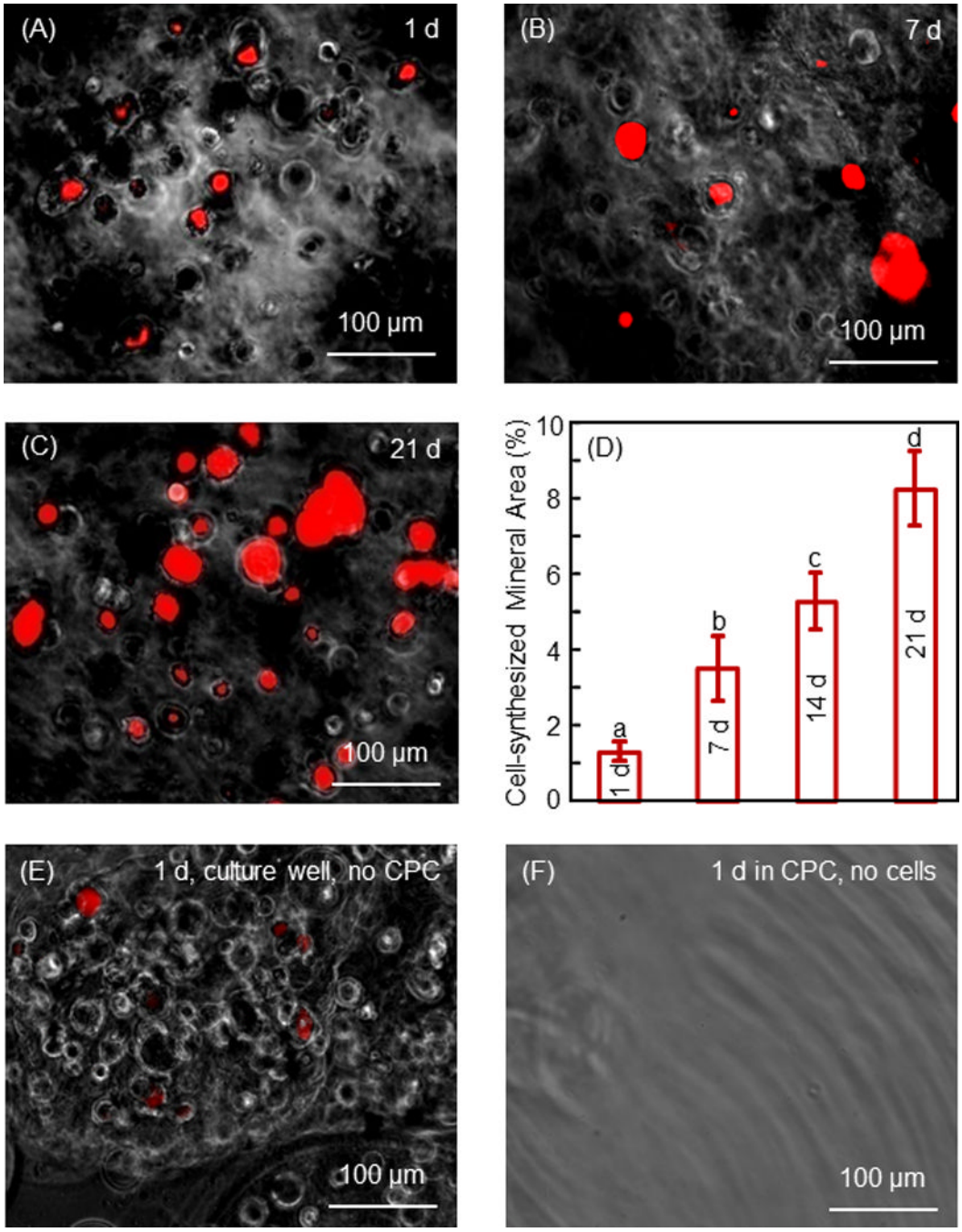

Figure 6.

Mineral synthesis by hESC-MSCs in hydrogel microbeads in CPC. Xylenol stained minerals into a red color for (A–C) 1 d, 7 d and 21 d, respectively. (D) The percentage of mineralization area stained in red. Each value is mean ± sd (n = 6). Values with dissimilar letters are significantly different from each other ($p < 0.05$). Mineral synthesis by the encapsulated hESCd-MSCs was increased by 7-fold in 21 d. (E) Microbeads with cell encapsulation were cultured for 1 d in cell culture well without CPC. (F) Microbeads without cells were placed in CPC for 1 d. The microbeads were then collected for xylenol staining. These results confirmed that the red staining in A–C was from the cells and not from CPC.

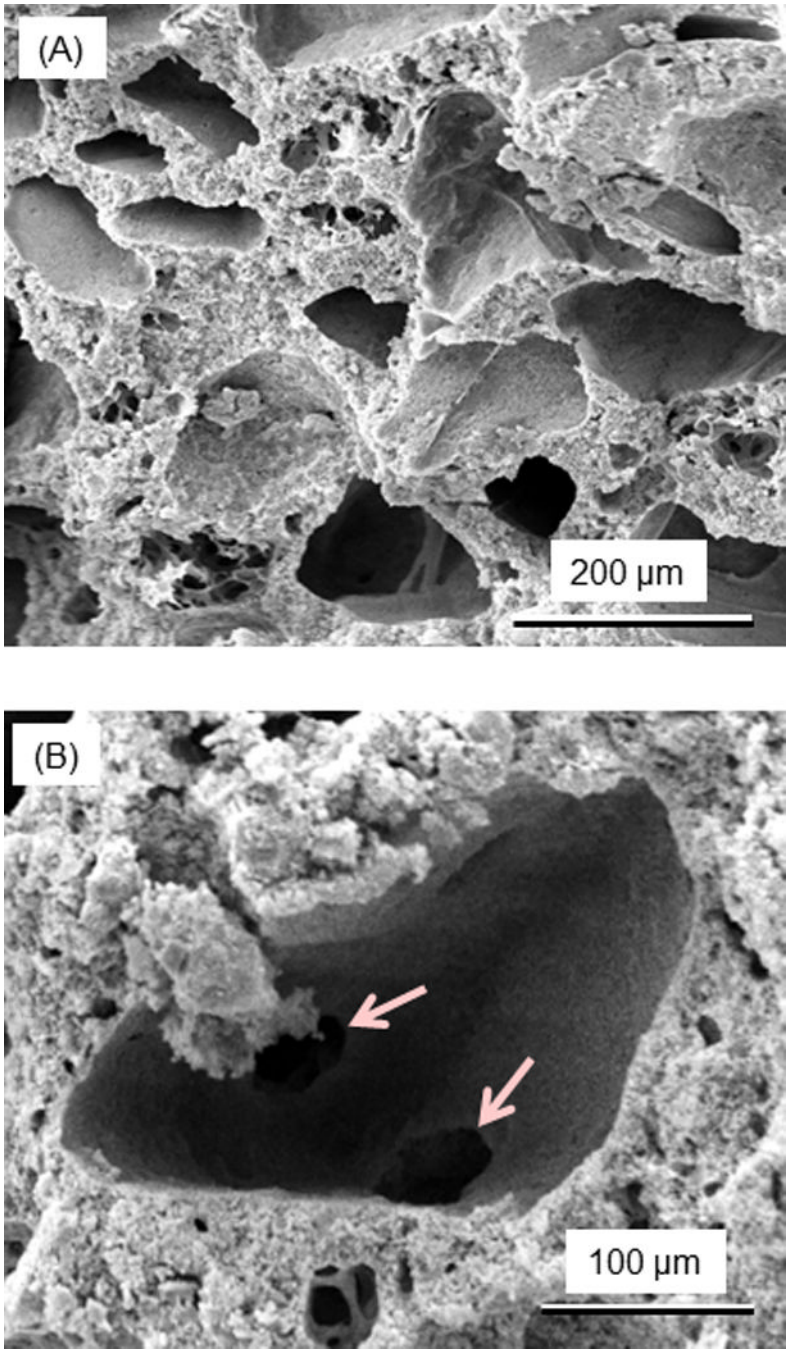

Figure 7.
SEM micrographs of the porosity in CPC scaffold. (A) After the dissolution of mannitol porogen by immersion for 1 d, macropores in CPC were created in the shapes of the entrapped mannitol particles. (B) Examples of pore interconnection, with arrows indicating the open connections in the bottom of a macropore. The macropore size in CPC ranged from approximately 50 to 343 μm, with an average of 218 μm.